ULTRASONIC IMAGING **23,** 90- 105 (2001)

Feasibility Study of Time-Intensity-Based Blood Flow Measurements Using Deconvolution

CHIH- KUANG YEH, SHENG- WUEI WANG AND PAI- CHI LI

Department of Electrical Engineering
National Taiwan University
Tapei, Taiwan, R.O.C.
email: paichi@cc.ee.ntu.edu.tw

Ultrasonic contrast agents have been used to enhance the acoustic backscattered intensity of blood and to assist the assessment of blood flow parameters. One example is the time-intensity method based on the indicator-dilution theory. In this case, a mixing chamber model can be employed to describe the concentration of the contrast agent as a function of time. By measuring the time intensities at both the input and output of the blood mixing chamber, blood flow information can be obtained if proper deconvolution techniques are applied. Note that most deconvolution techniques assume a linear and time invariant (LTI) system for the mixing of the contrast agent with blood. In this paper, the hypothesis that a blood mixing chamber is an LTI system was tested. Several aspects were studied. One aspect was the linear relationship between the concentration of the contrast agent and the backscattered intensity. The other aspect was the dependence of the derived time constants on the concentration. The concept of an effective mixing volume was also introduced and evaluated. Finally, the input and the output time constants were measured and compared to theory under the LTI assumption. Extensive experiments were performed. Two *in vitro* flow models were constructed and two contrast agents were used. Results indicated that the LTI assumption does not hold and quantitative flow estimation is generally not possible. Nonetheless, the indicator-dilution theory can still be applied if only relative measurements of the flow rate are required.

KEY WORDS: Blood flow estimation; deconvolution; effective mixing volume; time-intensity curve; ultrasonic contrast agent.

1. INTRODUCTION

Ultrasonic contrast agents are used to enhance the acoustic backscattered intensity of blood. They improve blood flow detection and offer possibilities to visualize perfusion conditions. Several recent studies have focused on *in vivo* and *in vitro* flow measurements based on the indicator-dilution theory.[1-6] The indicator-dilution theory provides a mathematical model for estimating hemodynamic parameters using changes in the backscattered intensity as a function of time (i.e., the time-intensity curve).[7-11] It has been shown that relative change in the wash-out rate of the time-intensity curve is linearly proportional to the volumetric flow rate.[5] It has also been shown that the peak intensity of the time-intensity curve is approximately linearly proportional to the volume concentration of the injection contrast agent.[12] Thus, the possibility for quantitative perfusion analysis using the time-intensity curve has been demonstrated.

The concentration of the contrast agent as a function of time can be mathematically derived by modeling the flow system as a series of blood mixing chambers. Each mixing chamber is described by a transfer function relating the indicator concentration entering (i.e., input) and leaving (i.e., output) the chamber as a function of time. With a bolus injection, a good correlation between time constants derived from the time-intensity curve and the volumetric flow rate can generally be found, if the acoustic intensity is linearly proportional to the concentration.[4] However, the time-intensity based methods are not as effective when the in-

0161-7346/01 $18.00

jection site is far away from the measurement site.[12] The situation can be viewed as the case where there are more than one mixing chamber between the injection site and measurement site. Thus, the input function of the last mixing chamber has a prolonged duration. When a prolonged injection is introduced, the output time-intensity curve reflects not only the dilution process in the mixing chamber, the input must also be taken into account.

To take into account the input function, the output time-intensity curve of the mixing chamber can be represented as the convolution of the input function and transfer function of the mixing chamber.[13-16] Assuming a linear and time-invariant (LTI) system, the transfer function of the mixing chamber can be obtained by deconvolution techniques if both the input and the output time-intensity curves are available. However, most deconvolution algorithms proposed to date were applied to analyze simulation data. Efficacy of the deconvolution algorithms on *in vitro* and *in vivo* data is not yet evaluated.

A fundamental hypothesis that needs to be tested before investigating the deconvolution techniques is the assumption that the blood mixing chamber is LTI.[17] In other words, it is necessary to verify if the acoustic backscattered intensity is linearly proportional to the concentration such that the measured time-intensity curve reasonably represents the temporal change of the concentration of the contrast agent. Influence of the concentration on flow estimation has been previously discussed.[2-3, 11-12] The linear relationship between the concentration and parameters such as the area under the time-intensity curve and the peak intensity was found if the concentration was within a certain range. One primary purpose of this study is to investigate not only the relationship between the acoustic intensity and the concentration, but also effects of the concentration on flow estimation results. In addition, both a compartment flow model and perfusion flow model will be used.

Another factor affecting the LTI assumption is the effect of the chamber size on blood mixing. In other words, the effective volume may be different from the physical volume of the mixing chamber.[18] If the contrast agent does not mix completely with liquid within the mixing chamber, the effective dilution volume is smaller than the physical volume of the mixing chamber. Because the wash-out rate of the contrast agent depends on both the volumetric flow rate and the volume of the mixing chamber, quantitative flow estimation is not possible without the knowledge of the effective mixing volume. In other words, the indicator-dilution theory can only be used to estimate the effective volume, instead of the physical volume. Influence of the effective volume on the time-intensity based flow estimation is also studied in this paper.

Finally, another purpose of this study is to investigate the validity of the LTI assumption by comparing the input time constant to the output time constant. The relationship between the input time constant and the output time constant are mathematically derived and compared to the measurement results. The experiments in this study were performed with both a compartment model and a perfusion model.[19] Each model had two configurations for bolus injections and prolonged injections, respectively. Experimental results are summarized with a discussion on the applicability and limitations of the time-intensity based flow estimation techniques.

2. MATERIALS AND METHODS

A. Basic principles

When a certain amount of indicator solution is input into the flow system, the concentration at the system output can be described based on the indicator-dilution theory. However, the concentration of the ultrasonic contrast agent is not directly measured in practice. In-

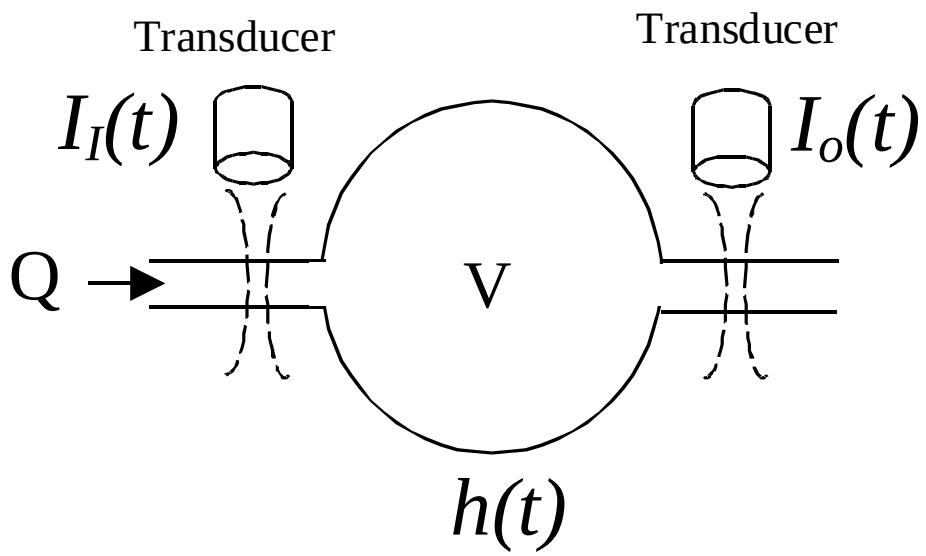

FIG. 1. Illustration of the input and the output of a mixing chamber.

stead, the backscattered acoustic intensity is used to represent the concentration of the contrast agent. The following discussion on the mixing chamber model assumes that the backscattered intensity is a linear function of the concentration of the contrast agent. The validity of this assumption will be studied in the next section.

A diagram of the mixing chamber is depicted in figure 1. The echo intensity measured at the output of a mixing chamber, denoted by $I_o(t)$, depends on the input function $I_i(t)$ and the transfer function $h(t)$. If the system is LTI, the output function can be expressed as the convolution of the input function and transfer function of the mixing chamber.[1] In other words,

$$I_O(t) = I_I(t) \otimes h(t), \tag{1}$$

where $\otimes$ stands for convolution and $h(t)$ is the transfer function of the mixing chamber. The transfer function $h(t)$ contains characteristics of the mixing chamber and is given by

$$h(t) = \begin{cases} 0 & t < 0 \\ \frac{1}{\tau} e^{-t/\tau} & t > 0 \end{cases} \tag{2}$$

where τ is considered as the system's transit time (i.e., inverse of the wash-out rate) and is proportional to the mixing chamber volume and inversely proportional to the volumetric flow rate.[1] Equation (1) indicates that deconvolution techniques can be applied to estimate the transfer function of a mixing chamber if both the input and the output time-intensity curves are available. After the transfer function is determined, blood flow parameters, such as the wash-out rate, can then be obtained.

The time-intensity curve is used to derive two parameters in this study. One is the mean transit time (MTT) and the other is the area under curve (AUC). The MTT is defined as

$$MTT = \frac{\int_0^\infty tx(t)dt}{\int_0^\infty x(t)dt}, \tag{3}$$

where $x(t)$ is either the measured time-intensity curve or the derived transfer function of the mixing chamber. The MTT represents the time for the entire fluid volume to pass though the mixing chamber. According to the indicator-dilution theory, there is an inverse relation between the flow rate and the MTT. If the transfer function is defined in Eq. (2), it can be shown that

$$MTT = \tau = \frac{V}{Q}, \tag{4}$$

where V is the volume of mixing chamber and Q is the volumetric flow rate. In this study, the flow rate ranged from 500 to 1100 ml/min and the size of the mixing chambers ranged from 200 to 930 ml.

Based on Eqs. (1) and (2), it can also be shown that the MTT of the output function (MTT_{out}) equals the sum of the MTT of the input function (MTT_{in}) and the MTT of the transfer function of mixing chamber (MTT_{mix}).[15] In other words,

$$MTT_{out} = MTT_{in} + MTT_{mix}. \tag{5}$$

To verify the LTI assumption, the MTT derived from Eq. (5) will be compared with the value derived from Eq. (4).

Finally, the AUC defined as the following equation is used to test the linear relationship between the concentration and backscattered intensity.[2]

$$AUC = \int_0^\infty I_o(t)dt \tag{6}$$

B. Experimental setup

Two *in vitro* flow models were constructed. One was made of a spherical compartment phantom and the other was made of a perfusion phantom.[19] Furthermore, each flow model had two different configurations. One was for bolus injection and the other was for prolonged injections. Figure 2 shows a single compartment phantom and figure 3 shows two compartment phantoms in cascade. If the input has a short duration compared to the MTT of the mixing chamber, the output intensity curve measured from the phantom shown in figure 2 approximates the transfer function of the mixing chamber (i.e., the input is approximated as an impulse). For the flow model shown in figure 3, on the other hand, the input of chamber A is also the output of chamber B. Thus, the time-intensity curve measured at the output of chamber A can be used to evaluate the time-intensity based method when the input has a prolonged duration.

The compartment phantom was made of an acrylic hollow sphere. Two silicon tubes connecting to the sphere were fixed in parallel with opposite flow directions and immersed in a

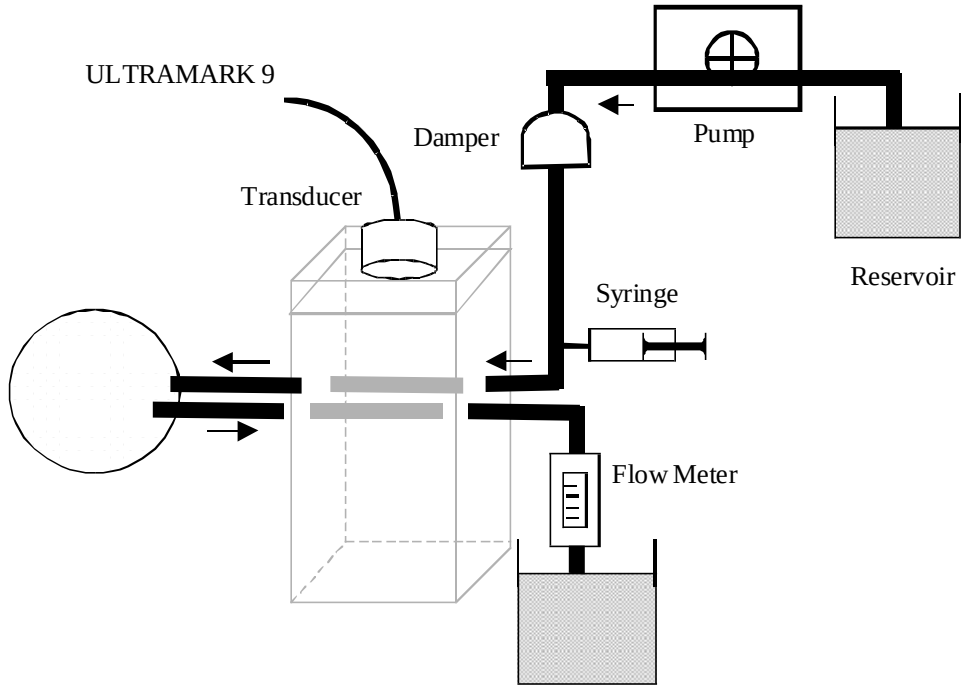

FIG. 2. Experimental setup for the compartment phantom.

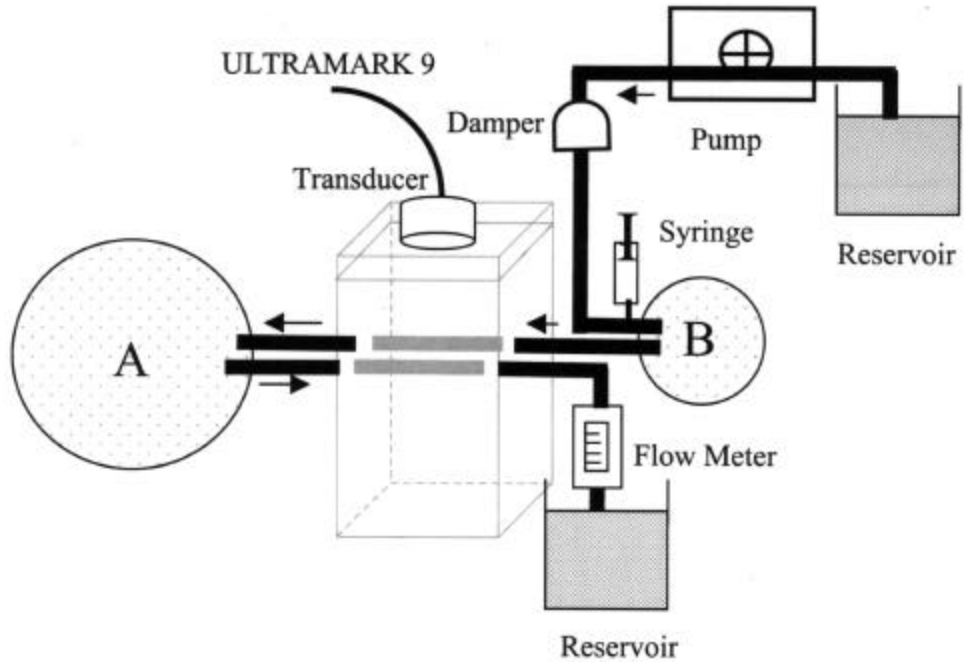

FIG. 3. Experimental setup for two compartment phantoms in cascade.

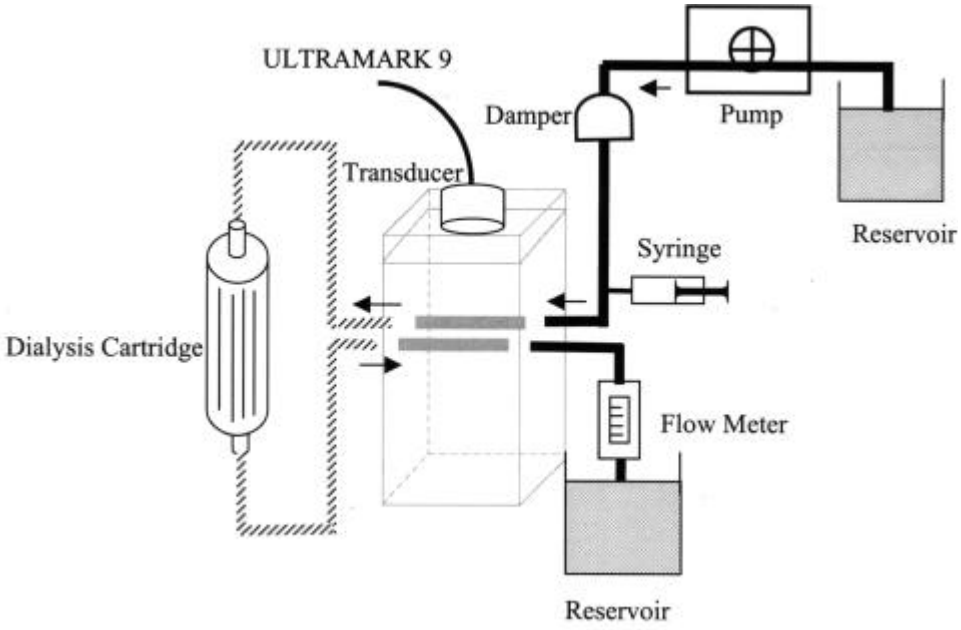

FIG. 4. Experimental setup for the perfusion phantom.

water tank. The diameter of the tubes was 8 mm. A 7-MHz linear array transducer (L7-4, Advanced Technology Laboratories, Bothell, WA, U.S.A.) was placed 2 cm above the tubes. The damper was used to stabilize the flow. To prevent recirculation of the contrast agent back into the phantom, the water in this system only passed through the model once. In figure 2, the contrast agent was injected to the tube at the front side of the sphere by a syringe. In figure 3, the injection position was at the input side of chamber B. The input time-intensity curve of chamber A was the transfer function of chamber B if the duration of the input injection was sufficiently short.

The other flow model was based on a perfusion phantom made of a dialysis cartridge.[19] Again, an additional sphere was inserted between the injection site and the perfusion phantom as the configuration for prolonged injections. Schematic diagrams of the two configurations are shown in figures 4 and 5, respectively. The dialysis tube (C-12, TERUMO Co., Tokyo, Japan) consisted of 8600 capillaries with a diameter of 200 μm and a length of 235 mm for each capillary, making a total volume of 79 ml.

C. Imageprocessing

The input and the output time-intensity curves were simultaneously measured using a commercial ultrasound machine (Ultramark 9, Advanced Technology Laboratories Inc., Bothell, WA, U.S.A.). The mechanical index (MI) was 0.7 with the imaging frame rate ranging from 20 to 30 Hz. The destruction of microbubbles due to the acoustic power level was negligible based on the fact that the ratio of the input AUC to the output AUC was close to unity in all cases. Effects of postprocessing on the time intensities were also ignored because the images were acquired prior to the postprocessing functions were applied. In addition, shadowing and other unwanted effects potentially resulting from the uneven microbubble

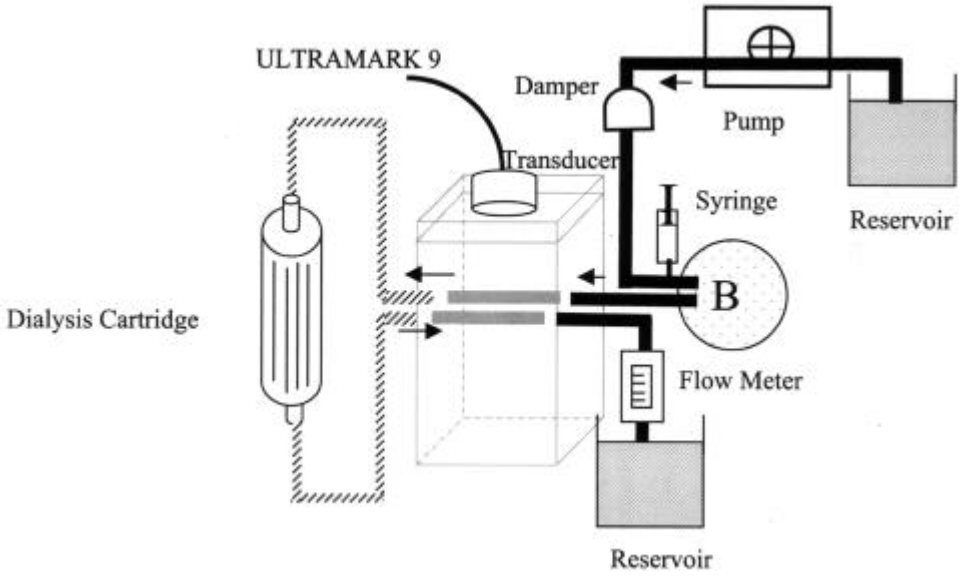

FIG. 5. Experimental setup for the perfusion phantom in cascade with a compartment phantom.

distribution were not observed in the gray-scale images. Gray-scale images of the transverse view of the input and the output tubes were acquired one frame per second. A total of 300 image frames (i.e., 5 minutes) were acquired and digitized by a frame grabber (UPG401B, UPMOST Corp., Taipei, R.O.C.) and stored for off-line analysis. The image size was 153 by 232 pixels covering a 36 mm by 55 mm area. A typical image is shown in figure 6. The two regions of interest denoted by the two circles correspond to the input and the output tubes. The image data were converted from the logarithmic scale to the linear scale before the mean backscattered intensities inside the ROI were calculated.

To obtain a time-intensity curve, a circle was used to cover the inner portion of the tube. The intensities of the pixels inside the ROI were summed and the result was used as the intensity at that particular time. The procedures continued until all the 300 digitized gray-scale images were processed.

To reduce noise in the time-intensity measurements, the time-intensity curve is fitted to a gamma function $g(t)$ defined as the following

$$g(t) = \alpha(t - t_o)^{\gamma} e^{-\beta(t - t_o)}, \tag{7}$$

where t_0 indicates a delay time, α and β are scaling factors and γ represents the skewness. All flow-related parameters were calculated after gamma function fitting. Typical input and output time-intensity curves are shown in figure 7. Note that the dotted lines correspond to the original measurements and the solid lines are with curve fitting.

D. Contrast agents

A commercial contrast agent (Levovist,® Schering, Berlin, Germany) and a self-made contrast agent were used. The self-made agent was made from human albumin using the agi-

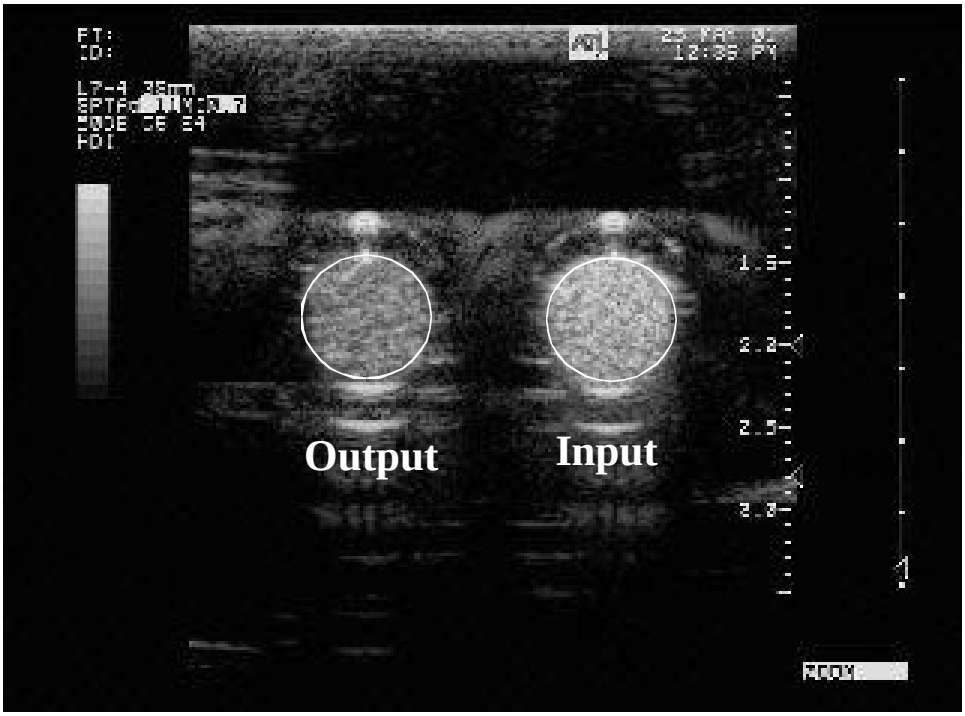

FIG. 6. A typical gray-scale image showing intensities from both the input and the output tubes.

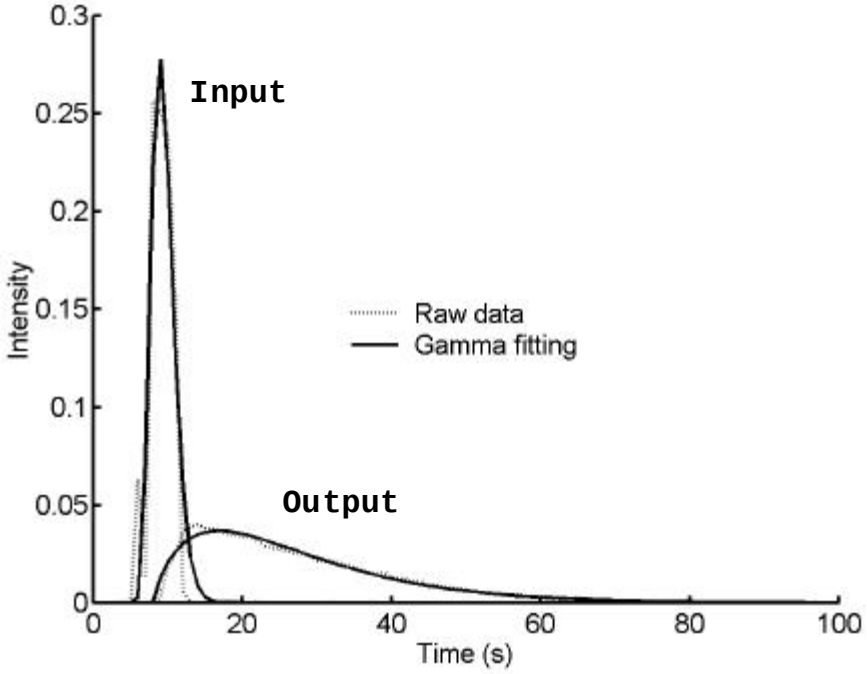

FIG. 7. Typical input and output time-intensity curves with (solid) and without (dotted) gamma fitting.

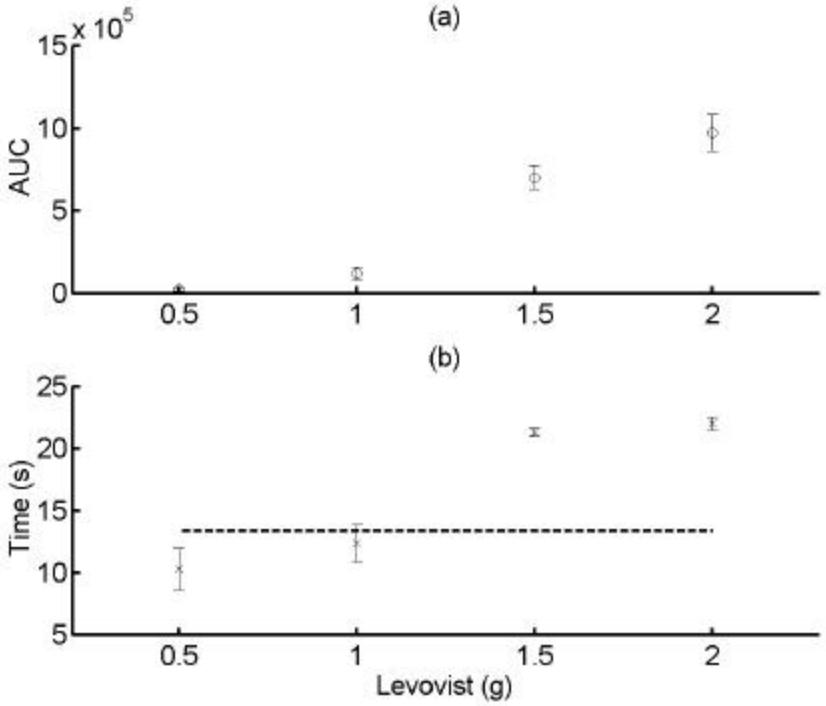

FIG. 8. (a) AUC of the in put time-intensity curve and (b) MTT of the out put time-intensity curve vs. Levovist® con cen tra tion for the com part ment phan tom.

tation technique.[4,20] The size of the self-made microbubbles was es ti mated us ing a light mi - cro scope (EMZ-TR, MEIJI Tech. Co., To kyo, Ja pan). The di am e ter of the self-made agent was about 20 to 50 mm.[4] The con cen tra tion of the al bu min-based con trast agent is pri mar ily de ter mined by the amount of air used when mak ing the agent.

3. EXPERIMENTAL RESULTS

A. Con cen tra tion vs. mean tran sit time

Experiments were conducted to evaluate influence of the concentration of the contrast agent on the MTT es ti mates. A flow rate of 900 ml/min was used. For each case, the av er age and the stan dard de vi a tion were taken from three in de pend ent mea sure ments. The ex per i - men tal setup is shown in fig ure 2, with the vol ume of the com part ment at 200 ml.

Figure 8(a) demonstrates the relationship between the AUC and the concentration of Levovist.® The av er age val ues are shown with the er ror bars rep re sent ing +/- one stan dard de vi a tion. Levovist® with four dif fer ent doses (0.5 g, 1.0 g, 1.5 g and 2.0 g) were mixed with 4 ml wa ter. It is shown that the AUC in creased with the Levovist® dose. Fig ure 8(b) shows the MTT es ti mated at four con cen tra tion lev els (i.e., four dif fer ent doses). Theoretical val - ues de rived from Eq. (4) were shown as the dashed line. Re sults in di cate that al though the AUC increased with the Levovist® concentration, the MTT estimates still varied with the concentration. The same experiments were also performed with the perfusion phantom shown in fig ure 4 un der the same ex per i men tal con di tions. Re sults are shown in fig ure 9.

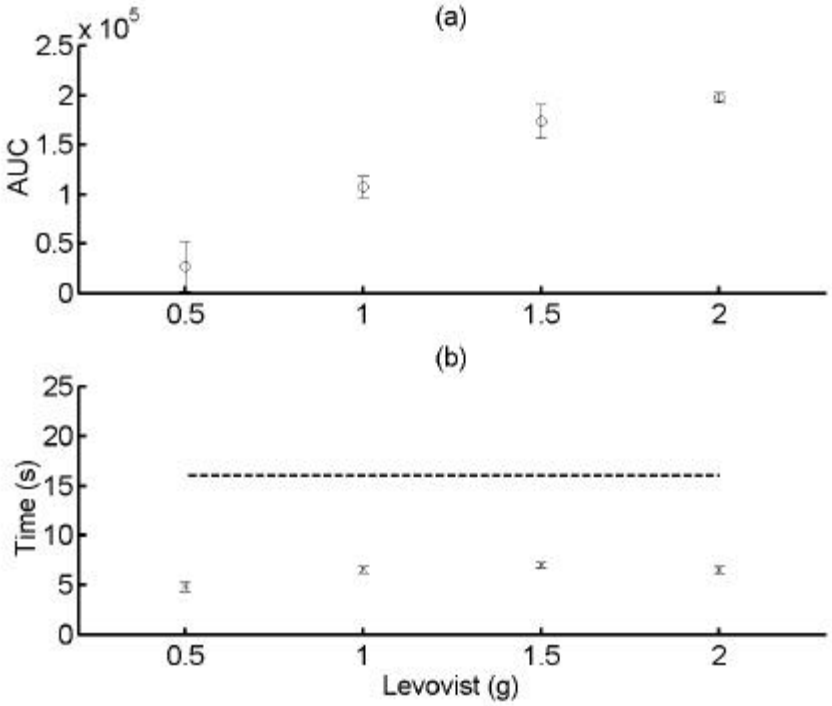

FIG. 9. (a) AUC of the input time-intensity curve and (b) MTT of the output time-intensity curve vs. Levovist® concentration for the perfusion phantom.

Again, the AUC increased with the Levovist® concentration, but the MTT estimates were all smaller than the theoretical value (dashed line). Note that the theoretical value was calculated based on the sum of the volume of the cartridge (79 ml) and the volume of the connecting tubes (160 ml). If only the volume of the cartridge was considered, the dashed line becomes much closer to the measurement results.

Note that the MTT's for the perfusion phantom (figure 9(b)) appear to be much flatter than those for the compartment phantom (figure 8(b)). One possible reason is the difference in the mixing chamber volume. In the perfusion phantom, the real dilution volume equaled the volume of the cartridge. The dilution volume of the compartment phantom, on the other hand, was larger than that of the perfusion phantom. In other words, the physical volume may be larger than the effective volume.

The experiments were also repeated using the albumin-based contrast agent. Four ml of water and 0.2 ml of 20% human albumin were used in all cases. The different concentration levels corresponded to 0.2, 0.4, 0.6 and 0.8 ml of air, respectively. Figures 10 and 11 show the results from the compartment phantom and perfusion phantom, respectively. In figures 10(a) and 11(a), the AUC increases with the amount of air. The amount of air primarily determines the concentration of the contrast agent. Figures 10(b) and 11(b) illustrate the MTT's estimated at different concentrations levels. Again, the MTT increased with the concentration for the compartment phantom and stayed relatively constant for the perfusion phantom.

Results shown in figures 8-11 indicate that the MTT generally depends on the concentration, although the measurements agree well with the theory in certain situations. In addition, the MTT estimates from the self-made agent have larger standard deviations than those from the commercial agent Levovist.® One possible reason is the size uniformity of microbubbles.

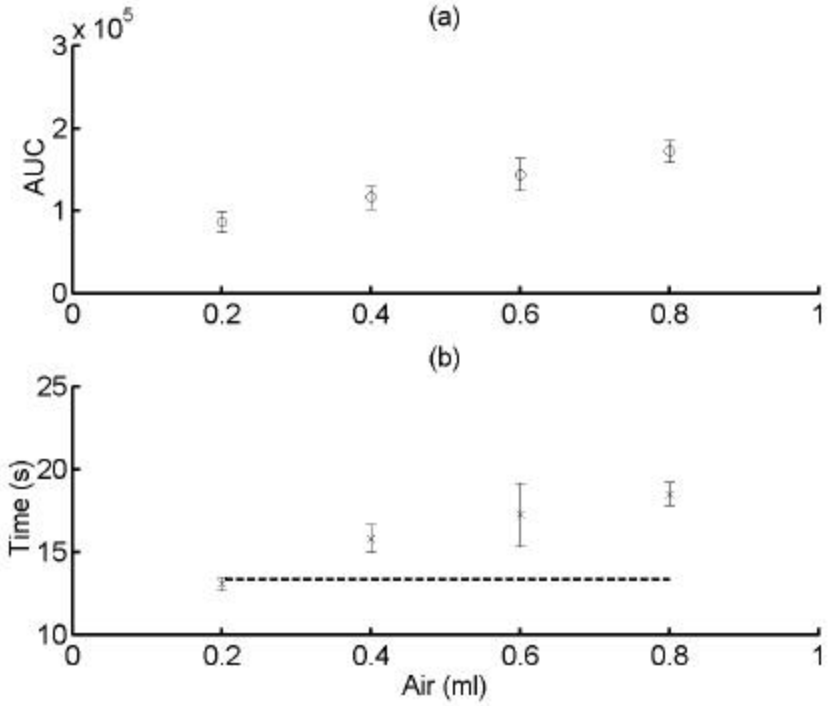

FIG. 10 (a) AUC of the in put time-intensity curve and (b) MTT of the out put time-intensity curve vs. concentration of the al bu min-based con trast agent for the com part ment phan tom.

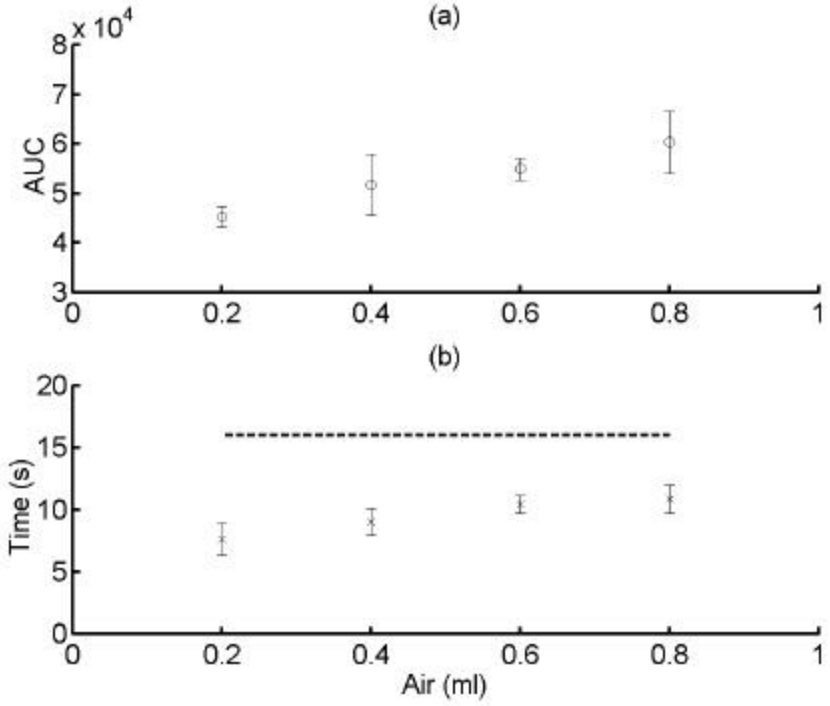

FIG. 11. (a) AUC of the in put time-intensity curve and (b) MTT of the out put time-intensity curve vs. concentration of the al bu min-based con trast agent for the per fu sion phan tom.

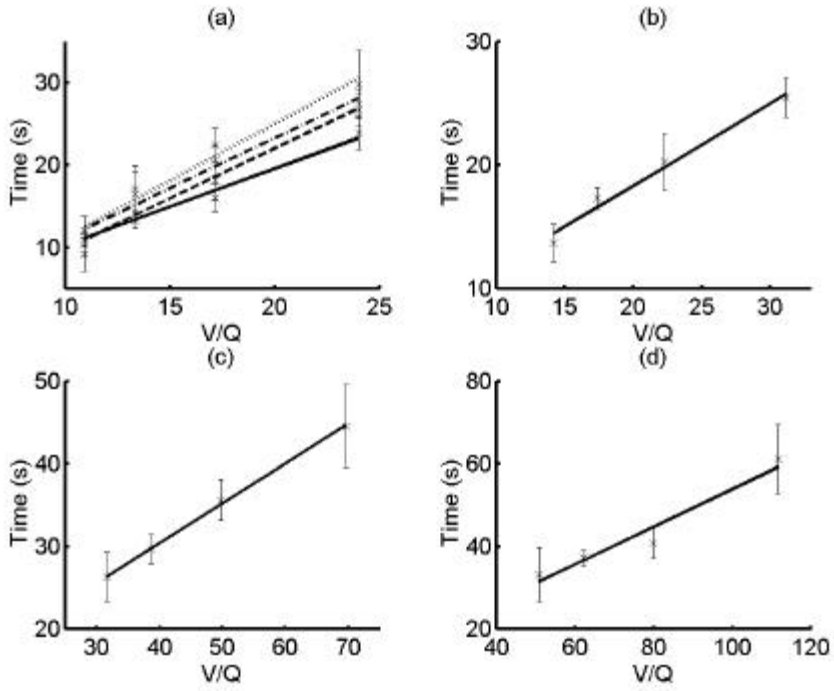

FIG. 12. MTT measured with the mixing chamber volume at (a) 200 ml, (b) 260 ml, (c) 580 ml, and (d) 930 ml. The air used for making the contrast agent was 0.2 ml for all solid lines. In (a), 0.4 ml of air was used for the dashed lines, 0.6 ml for the dot-dashed line and 0.8 ml for the dotted line.

For Levovist,® 99% of the microbubbles are smaller 4 μm whereas the size of the self-made agent ranged from 20 to 50 μm. The size uniformity may potentially affect the backscattered signal intensities.

B. Effective mixing volume

The MTT's were estimated from the output time-intensity curves using the compartment phantoms with different sizes and flow rates. The experimental setup is shown in figure 2 and the albumin-based contrast agent was used. Results are shown in figure 12. In figure 12(a), the MTT's obtained at different concentration levels were shown. Again, the four concentration levels corresponded to 0.2, 0.4, 0.6 and 0.8 ml of air, respectively. Four ml of water, 0.2 ml of 20% human albumin were used in all cases. The volume of the compartment phantom was 200 ml. Flow rates were 500, 700, 900 and 1100 ml/min. For each flow rate, five independent measurements were performed. The horizontal axis represents the theoretical values obtained from Eq. (4) and the vertical axis shows the measured MTT. Mean values are shown as crosses with the error bars corresponding to +/- one standard deviation. Linear regression was performed and the best-fit lines at different concentration levels are shown as the solid line (0.2 ml of air), the dashed line (0.4 ml of air), the dot-dashed line (0.6 ml of air) and the dotted line (0.8 ml of air). The four correlation coefficients between the MTT estimates and linear regression lines were 0.94, 0.92, 0.94 and 0.93, respectively. In all cases, the estimated MTT is approximately inversely proportional to the volume flow rate Q, demonstrating that the indicator-dilution theory can be applied for relative volumetric flow measurements. However, absolute measurements are not possible due to the different MTT estimated at different concentration levels.

TABLE 1. Summary of the estimated MTT's for four different volumes and four different flow rates. The volumes were (a) 200 ml, (b) 260 ml, (c) 580 ml, and (d) 930 ml.

	Flow rate	0.5 (l/min)	0.7(l/min)	0.9 (l/min)	1.2 (l/min)
(a)	**MTT (average)**	23.85	16.00	13.20	11.97
	V/Q	24.00	17.14	13.33	10.91
	κ	**0.99**	**0.93**	**0.99**	**1.10**
(b)	**MTT (average)**	25.48	20.39	17.31	13.72
	V/Q	31.20	22.29	17.33	14.18
	κ	**0.82**	**0.91**	**1.00**	**0.97**
(c)	**MTT (average)**	41.24	35.30	26.69	24.03
	V/Q	69.60	49.71	38.67	31.64
	κ	**0.59**	**0.71**	**0.69**	**0.76**
(d)	**MTT (average)**	61.11	40.86	37.26	33.18
	V/Q	111.60	79.71	62.00	50.73

Results shown in figures 12 (b) to 12 (d) correspond to the estimated MTT's at different flow rates and different volumes of the compartment. As in figure 12(a), the flow rates were 500, 700, 900 and 1100 ml/min. The compartment volume was 260 ml for figure 12(b), 580 ml for figure 12(c), and 930 ml for figure 12(d). The concentration of the contrast agent was fixed at 4 ml of water, 0.2 ml of 20% human albumin and 0.2 ml of air. The three correlation coefficients between the estimated MTT's and the best-fit lines were 0.94, 0.92 and 0.88, respectively. The slopes of linear regression the best-fit lines for figures 12(b) to 12(d) were 0.66, 0.48 and 0.45, respectively. The high correlation coefficients showed that relative flow estimation is possible with the time-intensity based methods. Moreover, it is shown that the slope decreased as the chamber volume increased. In other words, the effective mixing volume changed with the physical volume. As the physical volume increased, the ratio of the effective volume to the physical volume decreased.

The results at the 0.2 ml of air concentration level are summarized in table 1. Tables 1(a) to 1(d) include results corresponding to the compartment volume of 200, 260, 580 and 930 ml, respectively. In each case, the average estimated MTT's are shown in the second row. The theoretical values based on Eq. (4) and the ratios (κ's) of the estimated values to the theoretical values are shown in the third row and fourth row, respectively. If κ is close to one, it indicates that the contrast agent mixes with the fluid completely within the chamber and the indicator-dilution theory can be applied for absolute analysis. Otherwise, only relative measures can be obtained. As shown in table 1, κ is the closest to the one with the smallest volume. It decreases as the compartment volume increases.

C. Prolonged injections

The experimental setups shown in figures 3 and 5 were used to investigate effects of prolonged injection. For the setup shown in figure 3, the sizes of chambers A and B were 260 ml

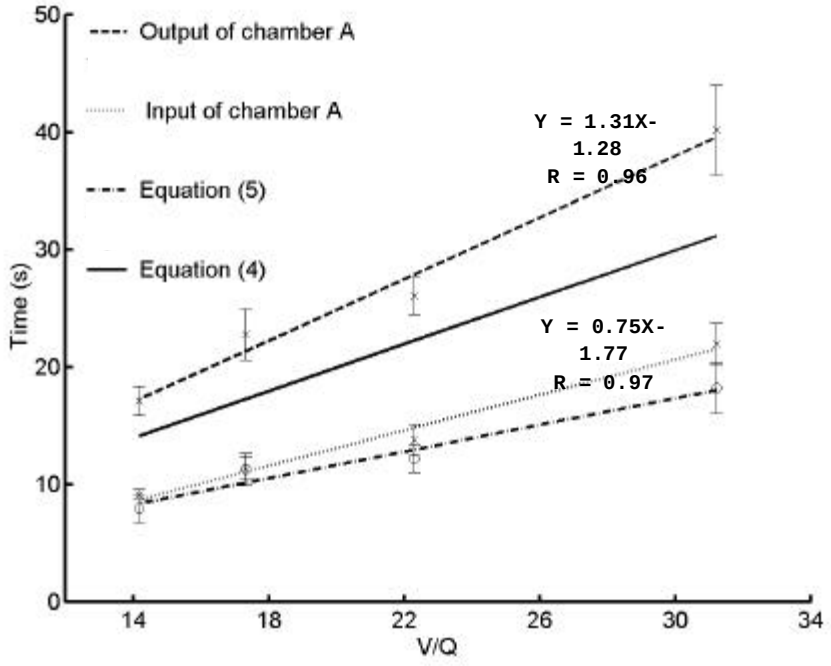

FIG. 13. Input and output MTT's measured with two compartment phantoms in cascade (setup shown in figure 3).

and 200 ml, respectively. Four flow rates at 500, 700, 900 and 1100 ml/min were used. At each flow rate, five independent measurements were performed to obtain mean and standard deviation. The self-made contrast agent composed of 0.2 ml of air, 4 ml of water and 0.2 ml of 20% human albumin was used.

Results are shown in figure 13. The horizontal axis represents the theoretical values obtained from Eq. (4) (i.e., 260 ml for chamber A divided by the flow rate) and the vertical axis corresponds to various MTT values. The dotted line and the dashed line are the best-fit lines for the input and output MTT's of chamber A based on the measured time-intensity curves. According to Eq. (5), the MTT for chamber A can be obtained by subtracting the input MTT from the output MTT. The results are shown as the dot-dashed line. The mixing chamber MTT can also be found according to Eq. (4) and results are shown as the solid line. Note that the solid line is simply a straight line with a slope of one. Apparently, the solid line is distinctly different from the dot-dashed line indicating that the concentration relationship described by Eq. (1) may not be valid.

The same experiments were performed with the setup shown in figure 5. The size of chamber B was 200 ml and the chamber A was replaced with a dialysis cartridge. Results are shown in figure 14. Similar to the results shown in figure 13, the convolution relationship between the input time-intensity curve and the output time-intensity curve again does not hold. Nonetheless, all the measurement results shown in figures 13 and 14 indicate that the MTT is approximately inversely proportional to the volume flow rate Q.

4. CONCLUSION

The hypothesis that mixing of the contrast agent is an LTI process was tested in this paper. Such a study is critical in determining if deconvolution techniques can be applied for quanti-

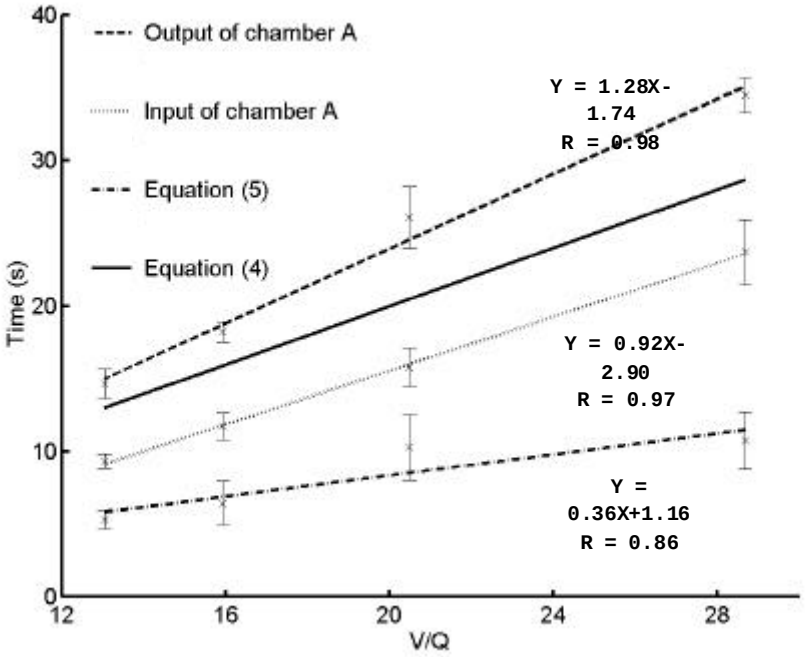

FIG. 14. Input and output MTT's measured with the perfusion phantom in cascade with a compartment phantom (setup shown in figure 5).

tative blood flow estimation. Results indicated that although the backscattered intensity increased with the concentration of the contrast agent, the measured MTT's also varied as the concentration varied. In addition, the MTT's of the mixing chamber derived based on Eq. (5) were different from the MTT's obtained based on Eq. (4). Therefore, it is concluded that the mixing process is generally not LTI and deconvolution techniques cannot be applied for measuring the absolute flow rate. Moreover, table I showed that the MTT estimates were affected by both the volume of the mixing chamber and the flow rate. In general, the MTT estimates were closest to the the ory with a smaller mixing chamber and at a higher flow rate. Although deconvolution techniques are generally not applicable, results in figures 12 to 14 showed that a linear relationship was still present between the measured MTT values and the oretical MTT values. Thus, time-intensity based methods are still feasible if only relative flow analysis is required.

In another study of this research project, the compartment flow phantom was placed both vertically and horizontally. Results showed that both configurations produced good relative estimates of flow parameters. Hence, influence of microbubbles buoyancy can be ignored when the larger diameter self-made agent was used.

Only constant flows were considered in this paper. In practice, pulsatile flows are present and the transfer function becomes time-varying since the time constant is also a function of the flow rate. Effects of the pulsatile flows on flow estimation need to be further studied. New methods based on both the input and the output time-intensity curves are also of great interest.

ACKNOWLEDGEMENTS

The authors would like to thank Dr. W. C. Yeh for his assistance on the experiments, and W. C. Tsai and T. Y. Chen for developing the image processing tool. This work was supported in part by National Science Council under grant NSC 89-2213-E-002-128.

REFERENCES

1. Chen, X., Schwarz, K., Phillips, D. et al, A mathematical model for the assessment of hemodynamic parameters using quantitative contrast echocardiography, *IEEE Trans. Biomed. Eng. 45*, 754-765 (1998).

2. Claassen, L., Seidel, G. and Algermissen, C., Quantification of flow rates using harmonic gray-scale imaging and an ultrasonic contrast agent: an *in vitro* and *in vivo* study, *Ultrasound Med. Biol. 27*, 83-88 (2001).

3. Heidenreich, P. A., Wiencek, J. G., Zaroff J. G. et al, *In vitro* calculation of flow by use of contrast ultrasonography, *J. Am. Soc. Echoc. 6*, 51-61 (1993).

4. Li, P. C., Yeh, C. K. and Wang, S. W., Time-intensity based volumetric flow measurement: an *in vitro* study, *Ultrasound Med. Biol.* (2001). (submitted)

5. Schwarz, K. Q., Bezante, G. P., Chen, X. et al, Volumetric arterial flow quantification using echo contrast. An *in vitro* comparison of three ultrasonic intensity methods: radio frequency, video and Doppler, *Ultrasound Med. Biol. 19*, 447-460 (1993).

6. Goldberg, B. B., *Ultrasound Contrast Agents*, Chapt. 3, pp. 21-42 (Dunitz ltd. London., 1997).

7. Ugolini, P., Delouche, A., Herment, A. et al, *In vitro* flow quantification with contrast agent, *Ultrasound Med. Biol. 26*, 113-120 (2000).

8. Wilkening, W., Helbeck, S., Postert, T. et al, Brain perfusion imaging using contrast agent specific imaging modes, in *Proc. IEEE Ultrasonic Symp.* , pp. 1721-1724 (1999).

9. Wilkening, W., Postert, T., Federlein, J. et al, Ultrasonic assessment of perfusion conditions in the brain and in the liver, in *Proc. IEEE Ultrasonic Symp.* , pp. 1545-1548 (2000).

10. Ostrander, L., Lee, B., Silverman, D. et al, *IEEE Trans. Biomed. Eng. 37*, 1017-1023 (1990).

11. Schwarz, K. Q., Bezante, G. P., Chen, X. et al, Quantitative echo contrast concentration measurement by Doppler sonography, *Ultrasound Med. Biol. 19*, 289-297 (1993).

12. Wilson, B., Shung, K. K., Hete, B. et al, A feasibility study on quantitating myocardial perfusion with Albunex®, an ultrasonic contrast agent, *Ultrasound Med. Biol. 19*, 181-191 (1993).

13. Mor-Avi, V., Akselrod, S., David, D. et al, Myocardial transit time of the echocardiographic contrast media, *Ultrasound Med. Biol. 19*, 635-648 (1993).

14. Gobbel, G. T. and Fike, J. R., A deconvolution method for evaluating indicator-dilution curves, *Phys. Med. Biol. 39*, 1833-1854 (1994).

15. Bates, J. H., Deconvolution of tracer and dilution data using the Wiener filter, *IEEE Trans. Biomed. Eng. 38*, 1262-1266 (1991).

16. Axel, L., Cerebral blood flow determination by rapid-sequence computed tomography: theoretical analysis, *Neuroradiology 137*, 679-686 (1980).

17. Eigler, N. L., Pfaff, J. M., Zeiher, A. et al, Digital angiographic impulse response analysis of regional myocardial perfusion: linearity, reproducibility, accuracy, and comparison with conventional indicator dilution curve parameters in phantom and canine models, *Circ. Res. 64*, 853-66 (1989).

18. Fred, S. G., Basic concepts in the determination of vascular volumes by indicator-dilution methods, *Circ. Res. X*, 429-446 (1962).

19. Hindle, A. J. and Perkins, A. C., A perfusion phantom for the evaluation of ultrasound contrast agent, *Ultrasound Med. Biol. 20*, 309-314 (1994).

20. Navin, C. N. and Reinhard, S., Advances in echo imaging contrast enhancement, Chapt. 3, pp. 21-4 (Kluwer Academic Publishers, 1993).